

Shading-based Shape Refinement of RGB-D Images

April 3, 2013

This is the supplementary material referred to in our paper. To best demonstrate the use of our recovered normals for 1) pointcloud refinement, 2) relighting and 3) 3D surface reconstruction, we also include a supplementary video where readers can view the results at different viewpoints. We kindly refer the readers to it.

1 Repairing Kinect Scenes

Here we display three additional Kinect scenes, *dog*, *jeans* and *couch* repaired by our approach. In *dog*, the shading information allows for subtle shape reconstruction as observed around the eye regions, the protruded nose region and the ear region where a hole is present in the input. In *jeans*, shape-from-shading correctly reveals the wrinkle details. In *couch*, patches repaired the *structural hole*, after which the whole object surface is refined with the addition of shading details both in the hole and the other regions.

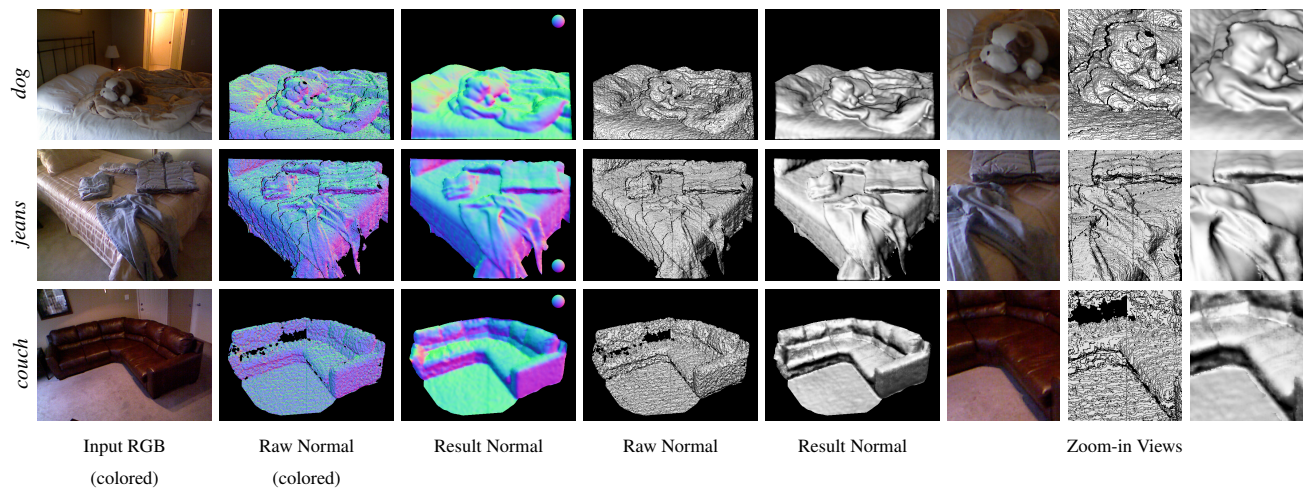


Figure 1: *Kinect scenes repaired by our approach.*

2 Comparison with Other Methods

Here we show one additional comparison with [1] on normal map estimation.

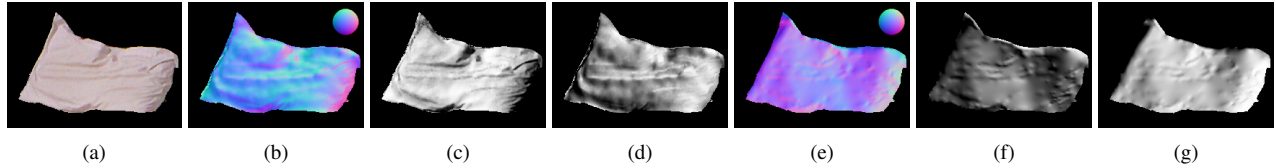


Figure 2: Comparison to SFS technique of [1]. (a) Input RGB image. (b-d) Our recovered normals and two normal maps \mathbf{N} shaded as $\mathbf{N} \cdot \mathbf{L}$ with $\mathbf{L} = (-\frac{1}{\sqrt{3}}, \frac{1}{\sqrt{3}}, \frac{1}{\sqrt{3}})^T$ and $\mathbf{L} = (\frac{1}{\sqrt{3}}, \frac{1}{\sqrt{3}}, \frac{1}{\sqrt{3}})^T$. (e-g) Recovered normals and shaded images of [1] using generic albedo and illumination priors. Note that our method also takes a noisy Kinect depth map as input.

3 Approach

In this section, we provide additional illustrations / implementation details of our approach to help reader with re-implementation of our method.

3.1 Data Structure

The following is an illustration of the bin data structure, $B_{u,j,k}$.

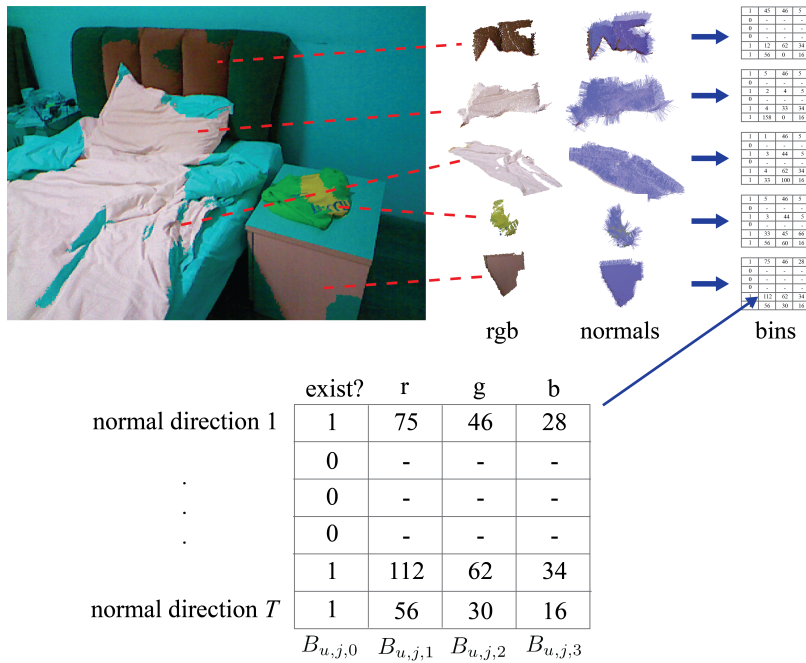


Figure 3: Example clusters. A cluster contains normals of different directions. Among different clusters, common bins (corresponding to common normal directions) are used for estimating the relative albedos.

3.2 Pseudocode

The following is pseudocode for the relative albedo estimation step.

Algorithm 1: Calculate All Relative Albedos

input : MST and starting cluster index s
output: Relative albedos of all clusters in MST, w.r.t starting cluster C_s

begin

- ┌ $a \leftarrow [1, 1, 1];$
- └ AlbedoDFS (s, a);

Procedure AlbedoDFS(i, b)

foreach edge $E_{i,j}$ **do**

- ┌ $rel \leftarrow \text{CalculateRelativeAlbedo}(i, j);$
- └ **for** $k \leftarrow 1$ **to** 3 **do**
 - ┌ $rel[k] \leftarrow rel[k] b[k];$
 - └ $p_{i,k} \leftarrow rel[k];$
- └ AlbedoDFS (j, b);

Function CalculateRelativeAlbedo(u, v)

input : Cluster indices u and v
output: RGB relative albedos of cluster C_v over cluster C_u

$count \leftarrow 0;$
// find common bins among T normal directions sampled on icosahedron

for $t \leftarrow 1$ **to** T **do**

- ┌ **if** $B_{u,t,0} \ \&\& \ B_{v,t,0}$ **then**
- └ $count \leftarrow count + 1;$

$ratios[1\dots count, 1\dots 3] \leftarrow 0;$
 $cur \leftarrow 1;$

for $t \leftarrow 1$ **to** T **do**

- ┌ **if** $B_{u,t,0} \ \&\& \ B_{v,t,0}$ **then**
- └ **for** $k \leftarrow 1$ **to** 3 **do**
 - ┌ $ratios[cur, k] \leftarrow \frac{B_{v,t,k}}{B_{u,t,k}};$
 - └ $cur \leftarrow cur + 1;$

$result \leftarrow \text{RANSAC}(ratios);$
return $result;$

4 Experimental Results

4.1 Ground Truth Comparison



Figure 4: *Input scene with a Lambertian ball used for ground truth normal estimation experiments in Section 4.2 of the main text.*

4.2 Lighting Estimation

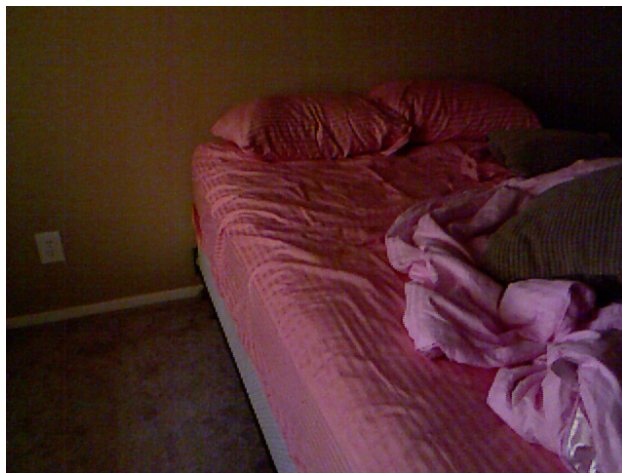


Figure 5: *Input scene used for lighting estimation experiments in Section 4.1 of the main text, and for the albedo normalization comparison with [2] in Section 4.4 of the main text.*

4.3 Omitting Costs

Here we show two additional results with the shape-from-shading cost term $\mathcal{E}_{sfs}(N)$ and the prior cost term $\mathcal{E}_{prior}(N)$ being omitted, respectively, and compare them with the results using all cost terms.

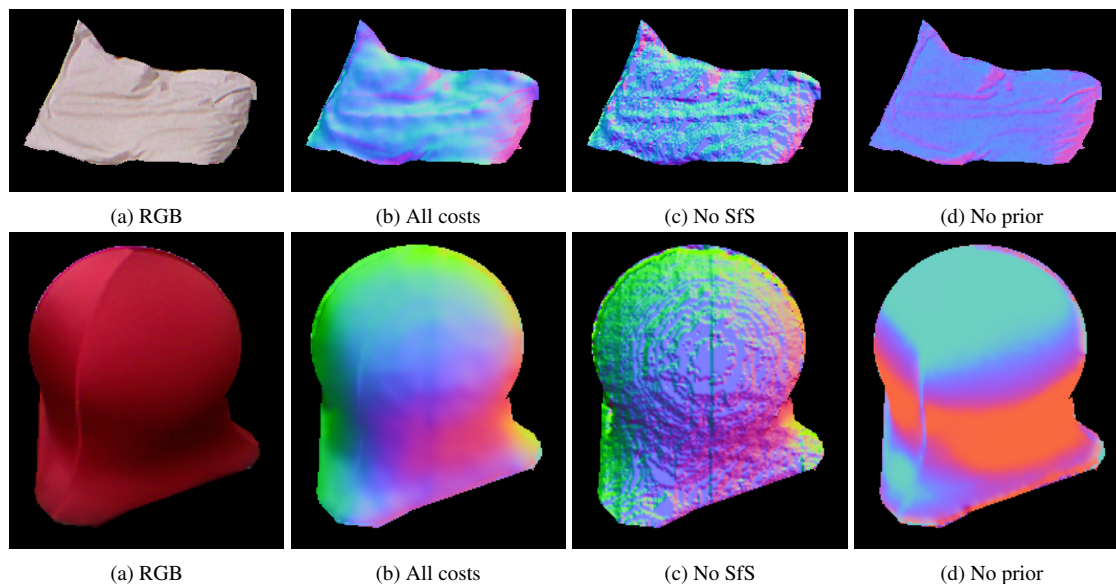


Figure 6: Above: results of omitting costs on pillow. Below: results on chair.

References

- [1] J. T. Barron and J. Malik. Color constancy, intrinsic images, and shape estimation. In *ECCV (4)*, pages 57–70, 2012.
- [2] K. J. Lee, Q. Zhao, X. Tong, M. Gong, S. Izadi, S. U. Lee, P. Tan, and S. Lin. Estimation of intrinsic image sequences from image+depth video. In *ECCV (6)*, pages 327–340, 2012.